In vivo Evaluation of ^{177}Lu- and $^{67/64}$Cu-Labeled Recombinant Fragments of Antibody chCE7 for Radioimmunotherapy and PET Imaging of L1-CAM-Positive Tumors

Jürgen Grünberg,[1] Ilse Novak-Hofer,[1] Michael Honer,[1] Kurt Zimmermann,[1] Karin Knogler,[1] Peter Bläuenstein,[1] Simon Ametamey,[1] Helmut R. Maecke,[2] and P. August Schubiger[1]

Abstract

Purpose: The L1 cell adhesion protein is overexpressed in tumors, such as neuroblastomas, renal cell carcinomas, ovarian carcinomas, and endometrial carcinomas, and represents a target for tumor diagnosis and therapy with anti-L1-CAM antibody chCE7. Divalent fragments of this internalizing antibody labeled with $^{67/64}$Cu and ^{177}Lu were evaluated to establish a chCE7 antibody fragment for radioimmunotherapy and positron emission tomography imaging, which combines high-yield production with improved clearance and biodistribution properties.

Experimental Design: chCE7F(ab′)$_2$ fragments were produced in high amounts (0.2 g/L) in HEK-293 cells, substituted with the peptide-linked tetraazamacrocycle 3-(*p*-nitrobenzyl)-1,4,7,10-tetraazacyclododecane-1,4,7,10-tetraacetate-triglycyl-L-*p*-isothiocyanato-phenylalanine, and labeled with ^{67}Cu and ^{177}Lu. *In vivo* bioevaluation involved measuring kinetics of tumor and tissue uptake in nude mice with SK-N-BE2c xenografts and NanoPET (Oxford Positron Systems, Oxford, United Kingdom) imaging with ^{64}Cu-3-(*p*-nitrobenzyl)-1,4,7,10-tetraazacyclododecane-1,4,7,10-tetraacetate-triglycine-chCE7F(ab′)$_2$.

Results: The ^{177}Lu- and ^{67}Cu-labeled immunoconjugates reached maximal tumor accumulation at 24 hours after injection with similar levels of 12%ID/g to 14%ID/g. Blood levels dropped to 1.0%ID/g for the ^{177}Lu fragment and 2.3%ID/g for the ^{67}Cu fragment at 24 hours. The most striking difference concerned radioactivity present in the kidneys, being 34.5%ID/g for the ^{177}Lu fragment and 16.0%ID/g for the ^{67}Cu fragment at 24 hours. Positron emission tomography imaging allowed clear visualization of s.c. xenografts and peritoneal metastases and a detailed assessment of whole-body tracer distribution.

Conclusions: $^{67/64}$Cu- and ^{177}Lu-labeled recombinant chCE7F(ab′)$_2$ revealed suitable *in vivo* characteristics for tumor imaging and therapy but displayed higher kidney uptake than the intact monoclonal antibody. The ^{67}Cu- and ^{177}Lu-labeled immunoconjugates showed different *in vivo* behavior, with $^{67/64}$Cu-3-(*p*-nitrobenzyl)-1,4,7,10-tetraazacyclododecane-1,4,7,10-tetraacetate-triglycine-F(ab′)$_2$ appearing as the more favorable conjugate due to superior tumor/kidney ratios.

At the present time, more than 10 antibody drugs are approved by the Food and Drug Administration for therapy of a variety of human diseases, including cancers (1). A few antibodies have been approved in radiolabeled form for tumor imaging and therapy, and this number may increase as new cancer-associated target antigens are found. The cell surface protein L1-CAM is a target antigen that plays a role in cell proliferation (2) and is emerging as a promising marker for cancers, such as neuroblastoma, renal cell carcinomas (3), and melanomas (4), as well as for ovarian and endometrial carcinomas (5). The chimeric monoclonal antibody chCE7 binds with high affinity to L1-CAM, is internalized into target tumor cells, and has been useful in radioimmunodiagnosis of metastatic neuroblastoma (6). For effective radioimmunotherapy, optimal tumor targeting is necessary to achieve therapeutic levels of the chosen radionuclides at the tumor site. Divalent antibody fragments, such as "minibodies" (7, 8), domain-deleted antibodies (9–11), or F(ab′)$_2$ fragments (12), are tumor-targeting agents that combine high accumulation at the tumor site comparable with intact antibodies, with more

Authors' Affiliations: [1]Center for Radiopharmaceutical Science ETH-PSI-USZ, Paul Scherrer Institute, Villigen, Switzerland and [2]Division of Radiological Chemistry, University Hospital Basel, Basel, Switzerland

Received 2/1/05; revised 4/7/05; accepted 5/4/05.

Grant support: Swiss National Science Foundation grant 3100A0-100200.

The costs of publication of this article were defrayed in part by the payment of page charges. This article must therefore be hereby marked *advertisement* in accordance with 18 U.S.C. Section 1734 solely to indicate this fact.

Requests for reprints: Ilse Novak-Hofer, Center for Radiopharmaceutical Science ETH-PSI-USZ, Paul Scherrer Institute, CH-5232 Villigen, Switzerland. Phone: 41-56-310-4067; Fax: 41-56-310-2849; E-mail: ilse.novak@psi.ch.

rapid clearance from the blood. However, in contrast to intact antibodies, antibody fragments have not been used frequently for radioimmunotherapy. In some cases, especially with small-sized monovalent fragments, this is due to unfavorable biodistributions with low tumor uptake and accumulation of radioactivity in the kidneys, but there are also disadvantages related to large-scale protein production of fragments. Monovalent and multivalent antibody fragments produced in bacteria are often characterized by poor solubility and tend to form aggregates, complicating their purification and further handling. Production of $F(ab')_2$ fragments by proteolytic cleavage of intact antibody leads to low yields. Production in mammalian cells avoids such problems, but low-producer cell lines make antibody production time consuming and expensive. We developed a system for producing high amounts of antibody fragments in mammalian cells (13), and in this study, we evaluate engineered $F(ab')_2$ fragments of anti-L1 monoclonal antibody (mAb) chCE7 with a view to their application in radioimmunotherapy and positron emission tomography (PET) imaging. In contrast to monovalent mAb chCE7 fragments, divalent fragments are internalized into target tumor cells and radioactivity from ^{67}Cu-labeled chCE7$F(ab')_2$ is retained intracellularly similarly to intact mAb chCE7 (14, 15), indicating the advantage of combining residualizing metallic nuclides with internalizing immunoconjugates (16–18). Radiometal-labeled antibodies have advantages over ^{131}I-labeled antibodies in terms of radiation doses delivered to tumors; consequently, ^{67}Cu-labeled (19–25) and, more recently, ^{177}Lu-labeled intact antibodies have shown promising results in animal models (18, 26) and in clinical trials (27). The choice of therapeutic nuclides for radioimmunotherapy depends on the size of targeted tumors. Both Monte Carlo simulations (28) and data from actual patient studies (29) show that the high energy of ^{90}Y and its long particle range make it suitable for irradiating large metastases, whereas medium-energy β^- emitters, such as ^{67}Cu and ^{177}Lu, are better suited for the irradiation of small-sized, disseminated metastases. The main physical difference between ^{67}Cu and ^{177}Lu nuclides, which emit β^- particles of similar energy, is their half-life of 2.6 and 6.7 days, respectively. A disadvantage of antibody fragments labeled with metallic radionuclides, including radiocopper, consists in the high uptake of radioactivity in the kidneys, due to retention of radiolabeled metabolites (30–32). For ^{177}Lu and ^{67}Cu labeling of $F(ab')_2$ fragments, we selected a peptide-linked chelator, which we had found to reduce kidney uptake of radiocopper-labeled antibody fragments (32). The kinetics of uptake in tumor xenografts and in normal tissues of ^{67}Cu and ^{177}Lu conjugates labeled with the triglycine-linked chelator were compared, and radiation doses to organs, such as kidney and liver, were evaluated. The purpose of this study was to investigate tumor and normal tissue uptake of ^{67}Cu- and ^{177}Lu-labeled recombinant $F(ab')_2$ fragments of anti-L1-CAM antibody chCE7 in SK-N-BE2c tumor-bearing mice to characterize their potential for treatment of L1-CAM-positive tumors. In addition, ultrahigh resolution PET imaging was done with ^{64}Cu-3-(*p*-nitrobenzyl)-1,4,7,10-tetraazacyclododecane-1,4,7,10-tetraacetate (DOTA)-triglycine–labeled $F(ab')_2$ fragments in two different murine tumor models to evaluate their potential for tumor imaging and to obtain a detailed regional distribution pattern in small structures, such as lymph nodes (33). The data support efforts to initiate clinical investigations with ^{67}Cu- and ^{64}Cu-labeled chCE7 antibody fragments.

Materials and Methods

Chemicals and solvents used were from Fluka (Buchs, Switzerland) unless stated otherwise. Fast protein liquid chromatography was done on a Pharmacia (Amersham Biosciences, Duebendorf, Switzerland) instrument (Pharmacia/LKB HPLC-pump 2248, Pharmacia/LKB controller LCC-2252 and Pharmacia/LKB UV detector UV-MII). A Berthold (Regensdorf, Switzerland) HPLC-LB 506A online radioactivity detector was used.

Cells and antibodies. HEK-293 cells were from the German Collection of Microorganisms (Braunschweig, Germany), SK-N-BE2c human neuroblastoma cells were from Instituto Nazionale per la Ricerca sul Cancro (Genova, Italy), and SKOV3 human ovarian carcinoma cells were a gift from Prof. P. Altevogt (German Cancer Center, Heidelberg, Germany). HEK-293 and SKOV3 cells were maintained in DMEM (4.5 g/L glucose) and SK-N-BE2c cells in MEM/Ham's F-12 (1:1) and 1% nonessential amino acids. All media were supplemented with 10% FCS, 2 mmol/L glutamine, 100 units/mL penicillin, 100 μg streptomycin, and 0.25 μg/mL fungizone. All media and additives were obtained from BioConcept (Allschwil, Switzerland).

chCE7 fragments. mAb chCE7 is a high-affinity, internalizing chimeric monoclonal antibody of the IgG1 subtype (human κ light chain and human γ1 heavy chain), which recognizes L1-CAM. Intact mAb chCE7 and chCE7 fragments were produced in HEK-293 cells and purified from cell culture supernatants as described (13).

Ligand substitution of monoclonal antibody chCE7 and chCE7F(ab')$_2$. DOTA-L-*p*-isothiocyanato-phenylalanine was purchased from Macrocyclics (Dallas, TX). Bifunctional 1-(*p*-nitrobenzyl)-1,4,7,10-tetraazacyclododecane-4,7,10-triacetate and triglycine–linked DOTA were synthesized according to published procedures (32). An aqueous solution (60 mmol/L; 7.5-30 μL) of the ligands (DOTA-L-*p*-isothiocyanato-phenylalanine and DOTA-triglycyl-L-*p*-isothiocyanato-phenylalanine) was added to 200 to 400 μL of 0.1 mol/L sodium phosphate buffer (pH 8) containing 1 mg (0.01 μmol) of chCE7$F(ab')_2$. The pH was adjusted using Na_3PO_4 (saturated solution) to 9 to 10 and the reaction mixture was incubated overnight (16 hours) at 4°C. Excess ligands was then removed by centrifugation-dialysis (Vivascience, Winkel, Switzerland) and buffer exchanged into 0.1 mol/L sodium citrate buffer (pH 5.5) for ^{67}Cu labeling and 0.25 mol/L ammonium acetate (pH 5.5) for ^{177}Lu labeling. The immunoconjugates were concentrated by centrifugation-dialysis to 1 to 2 mg/mL and stored at 4°C. The number of chelators coupled per $F(ab')_2$ molecule was estimated with an isotope dilution assay as described before (33).

Radiolabeling. ^{67}Cu was produced in-house by irradiating ^{nat}Zn with protons at the 72 MeV accelerator of the Paul Scherrer Institute (Villigen, Switzerland) as described before (34) and used for radiolabeling 1 day after production. For the PET imaging experiments, ^{64}Cu was produced at Paul Scherrer Institute as described before (33). ^{177}Lu was from IDB (Petten, the Netherlands) and used for radiolabeling 7 days after production.

Two hundred to 400 μg (250 μL) of the immunoconjugates in a total volume of 500 μL of 0.1 mol/L sodium acetate buffer (pH 5.5) or in 0.25 mol/L ammonium acetate buffer (pH 5.5) were reacted with 18.5 to 30 MBq (500-800 μCi) of neutralized ^{67}Cu solution or with 50 to 80 MBq ^{177}Lu solution. Labeling with ^{67}Cu was done for

30 minutes at 22°C and labeling with ^{177}Lu was done for 20 minutes at 37°C. After incubations, EDTA was added to a final concentration of 5 mmol/L for 5 minutes to complex unchelated copper or lutetium. Purification of the labeled antibodies was achieved by fast protein liquid chromatography size exclusion chromatography on a Superdex 200 column (Amersham Biosciences) in PBS buffer [0.1 mol/L NaCl, 0.05 mol/L sodium phosphate (pH 7.4)] with a flow rate of 1.0 mL/min. The F(ab′)$_2$ peak eluted with a retention time of 13 minutes.

Quality control of radiolabeled preparations. Immunoreactivity of labeled antibody conjugates was measured by cell-binding assays as described (35) and data were analyzed by the Lindmo and Bunn (36) method. Stability of the labeled antibodies after incubation in human plasma at 37°C was analyzed by fast protein liquid chromatography size exclusion chromatography on a Superdex 200 column in PBS buffer.

Animal studies. Animal studies were done in compliance with the Swiss laws on animal protection. Housing and animal husbandry was according to local law on animal protection. Nude mice (CD1-nu) from Charles River, Inc. (Sulzfeld, Germany) were used for the experiments. Growth of SKOV3 tumors was monitored in a pilot experiment by sequential PET imaging with ^{64}Cu-4-(1,4,8,11-tetraazacyclotetradec-1-yl)-methyl benzoic acid–labeled mAb chCE7 (33). Three nude mice, which had been injected i.p. with 5×10^6 SKOV3 human ovarian carcinoma cells, were imaged once weekly for a period of 3 weeks. Results showed that small metastases could be detected 2 weeks after inoculation and this time was chosen for imaging with ^{64}Cu-chCE7F(ab′)$_2$. S.c. tumors were generated by inoculating s.c. on one flank with 5×10^6 SK-N-BE2c human neuroblastoma cells suspended in 400 μL medium [MEM/Ham's F-12, 10% FCS, 2 mmol/L glutamine, and 1% nonessential amino acids (BioConcept), including 50% Matrigel HC (BD Biosciences, Allschwil, Switzerland)]. After 14 to 20 days when tumors had reached weights between 200 and 500 mg, ^{67}Cu- or ^{177}Lu-labeled immunoconjugates [100 μL, corresponding to 185 kBq (5 μCi), 5-10 μg F(ab′)$_2$] were injected i.v. into groups of four mice. At the indicated time points, animals were sacrificed and dissected. Tumors and organs were removed and measured together with an aliquot of the injected solution in a gamma counter using an energy window between 160 and 210 keV for ^{67}Cu and 15 to 600 keV for ^{177}Lu. Results are expressed as % injected dose per gram of tissue (%ID/g). Statistical analysis of data was done with Student's t test (two-tailed, unequal variance).

Positron emission tomography imaging. Radiocopper production by proton irradiation of ^{nat}Zn was modified to produce a larger amount of ^{64}Cu by changing the irradiation protocol as described (33). For the PET experiment, tumor mice were imaged using the dedicated small animal PET tomograph Nano-PET (Oxford Positron Systems, Oxford, United Kingdom) based on the Hierarchical Design and Characterization technology (36). The awake animals were lightly restrained and injected with 10 MBq (267 μCi, 130 μg) ^{64}Cu-DOTA-triglycine-F(ab′)$_2$ via a lateral tail vein. Twenty-one to 24 hours later, the animals were anesthetized and scanned as described before (33). PET data were acquired in list mode for 60 to 90 minutes and reconstructed in a single time frame using the OPL-EM algorithm (0.5 mm bin size, 200 × 240 × 240 matrix size; ref. 37). Image files were analyzed using the dedicated software Pmod (38).

Dosimetry. Dose calculations were done with the OLINDA software (39) using organ ratios human/mouse (g/g) of 901 for the kidney and 2,134 for the liver and assuming species-independent pharmacokinetics. The integral of the time activity curve was determined from the pharmacokinetic data in Tables 3 and 4. Data were extrapolated from 72 to 500 hours either assuming only the physical decay (T_{phys}) of the radionuclides or estimating a biological half-life (T_{biol}) based on the last three time points. The effective half-life was then calculated $1 / T_{eff} = 1 / T_{phys} + 1 / T_{biol}$.

Table 1. Physical properties of ^{67}Cu and ^{177}Lu

	^{67}Cu	^{177}Lu
β energies, keV		
Maximal	577	498
Mean	141	133
γ energies, keV (%)	93 (16)	113 (6)
	185 (48)	208 (10)
Half-life (d)	2.6	6.7

Results

Labeling of recombinant chCE7 fragments with ^{177}Lu and ^{67}Cu. Table 1 shows the physical characteristics of ^{67}Cu and ^{177}Lu (Table 1) and compares some features of labeling mAbs with these nuclides (Table 2). The amount of carrier lutetium or copper present in the isotope preparations influences the specific activity that can be achieved by labeling the immunoconjugates. At the present time, the specific activity of ^{177}Lu is higher than that of ^{67}Cu. In our study, the specific activity of the ^{177}Lu solution was 405 MBq/μg Lu at the time of antibody labeling (1 week after production). At this time, it was ~4-fold higher compared with the ^{67}Cu solution (112.5 MBq/μg Cu) at the time of antibody labeling, 24 hours after production). Carboxylated tetraazamacrocycles can be used for labeling with either Cu or Lu, as they chelate both metals rapidly under mild conditions and the resulting metal complexes show high *in vivo* stability (40). A difference of the resulting copper and lutetium immunoconjugates consists in the different charge of the metal complexes (negative for Cu, neutral for Lu) attached to mAb.

mAbs chCE7 and chCE7F(ab′)$_2$ were produced in high yields (0.1-0.2 g/L) in HEK-293 cells. Recombinant F(ab′)$_2$ fragments were engineered as histidine-tagged proteins and purified by a two-step procedure using Ni-affinity chromatography followed by size exclusion chromatography. Yields after purification were ~50% because of the coexpression of monovalent fragments (13). The DOTA- and triglycine-linked DOTA chelators were coupled to antibodies as isothiocyanato-derivatives (Fig. 1). Substitution of antibody fragments with the chelators and conditions for radiolabeling were similar for the two nuclides. Labeling yields of the ^{177}Lu-DOTA-F(ab′)$_2$ ranged between 40% and 70% and labeling yields of the DOTA-triglycine–linked F(ab′)$_2$ were consistently lower (6-30%) with both ^{67}Cu and ^{177}Lu. When the molar excess of DOTA-triglycyl-L-*p*-isothiocyanato-phenylalanine for conjugation was increased, the resulting conjugates did not show increased labeling yields; therefore, a molar excess of 45 was employed. About two DOTA-triglycine chelators were found to be attached per F(ab′)$_2$ using these conditions, which resulted in conjugates with good biodistributions. After labeling, a final concentration of 5 mmol/L EDTA was added and the conjugates were purified by fast protein liquid chromatography size exclusion chromatography to remove

Table 2. Some features of radiolabeling antibodies with ^{67}Cu and ^{177}Lu

	^{67}Cu	^{177}Lu
Nuclide availability	Limited	Good
Labeling procedures	Postlabeling, 30 min, 22°C	Postlabeling, 20 min, 37°C
Bifunctional chelators	CPTA-NHS,TETA (BAT) DO3A-NCS DOTA-triglycerine-NCS	DOTA-NCS DOTA-triglycerine-NCS PA-DOTA-NCS
Labeling yields (%)	30-70	30-70
Specific activities of mAbs (MBq/mg)	37.5-112.5	37.5-187.5

Abbreviations: CPTA, 4-(1,4,8,11-tetraazacyclotetradec-1-yl)-methyl benzoic acid; TETA, 6-(p-nitrobenzyl)-1,4,8,11-tetraazacyclotetradecane-1,4,8,11-tetraacetic acid; DOTA-NCS, DOTA-L-p-isothiocyanato-phenylalanine; DO3A-NCS, DO3A-L-p-isothiocyanato-phenylalanine; DOTA-triglycerine-NCS, DOTA-triglycyl-L-p-isothiocyanato-phenylalanine; PA-DOTA, 1-(1 carboxy-3-(p-nitrophenyl)prophyl)-1,4,7,10-tetraazacylclododecane-4,7,10-triacetate.

unbound radioactivity as well as small fragments. Immunoreactivity of ^{67}Cu- or ^{177}Lu-labeled fragments, as determined by cell-binding assays, was between 80% and 100%. Stability in human plasma at 37°C was analyzed by fast protein liquid chromatography size exclusion chromatography. Labeled fragments were stable in human plasma at 37°C for at least 48 hours, and no evidence of aggregation, fragmentation, or release of radioactivity was found (data not shown).

Effect of different chelators on biodistributions of ^{177}Lu-labeled mAb chCE7 and its F(ab′)$_2$ fragments in SK-N-BE2c tumor-bearing nude mice. chCE7 fragments were substituted using different amounts of the DOTA chelate to determine optimal labeling conditions. When the molar excess of DOTA/F(ab′)$_2$ was increased from 45 to 180, the number of chelators attached per F(ab′)$_2$ increased from 3 to 5. The immunoreactivity as measured by a cell-binding assay was found to be fully retained; however, biodistributions were strongly affected. Figure 2 shows biodistributions of ^{177}Lu-DOTA-chCE7F(ab′)$_2$ substituted with three and five chelators 24 hours after injection. The conjugate with the higher substitution ratio was characterized by drastically lower levels of radioactivity in the kidneys, high liver uptake, and low tumor uptake. In contrast, the conjugate with the lower substitution ratio shows higher tumor uptake and lower levels of activity in the liver. This conjugate is characterized by ~3-fold higher levels of radioactivity in the kidneys than in the tumor. When the DOTA-triglycine chelate we had employed previously for radiocopper labeling of antibody fragments was used for ^{177}Lu labeling, about two chelators were attached per F(ab′)$_2$. In contrast to previous results with ^{67}Cu-DOTA-triglycine-F(ab′)$_2$, no significant difference in radioactivity present in the kidneys was found 24 hours after injection with the ^{177}Lu-DOTA-triglycine conjugate (35.9 ± 8.45%ID/g compared with 34.48 ± 8.85%ID/g).

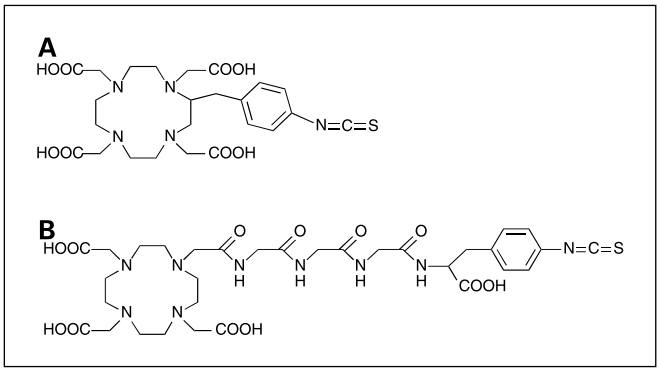

Fig. 1. Chelators used for ^{177}Lu and ^{67}Cu labeling of antibody fragments. *A*, DOTA-L-*p*-isothiocyanato-phenylalanine; *B*, DOTA-triglycyl-L-*p*-isothiocyanato-phenylalanine.

Comparative biodistribution of ^{177}Lu-DOTA-triglycine-F(ab′)$_2$ and ^{67}Cu-DOTA-triglycine-F(ab′)$_2$ in SK-N-BE2c tumor-bearing nude mice. The DOTA-triglycine–linked F(ab′)$_2$ conjugates were compared in ^{67}Cu- and ^{177}Lu-labeled form. Similar amounts (7.5-10 μg) of the conjugates were injected in nude mice with human neuroblastoma (SK-N-BE2c) xenografts and biodistributions were measured starting 2 hours after injection up to 72 hours. The results are summarized in Table 3 (^{177}Lu) and Table 4 (^{67}Cu). Both conjugates reached maximal tumor accumulation with similar levels of 12%ID/g to 14%ID/g at 24 hours after injection; differences were not statistically significant (P = 0.869). At 24 hours after injection, both conjugates showed ~3%ID/g uptake in control tumors (PC3 human prostate carcinoma cells), which do not express L1-CAM (data not shown). Figure 3 shows clearance of ^{67}Cu- and ^{177}Lu-labeled F(ab′)$_2$ from tumor and blood (Fig. 3A) and from the kidneys (Fig. 3B). Blood levels of the two conjugates dropped with a similar rate. Activity present in the blood reached at 24 hours 1.00 ± 0.79%ID/g for the ^{177}Lu conjugate and 2.30 ± 0.43%ID/g for the ^{67}Cu conjugate, the difference being significant (P = 0.001). The most conspicuous difference of the two conjugates was the clearance of radioactivity from the kidneys. Up to 8 hours, similar activities were observed in the kidneys, but at 24 hours and later ^{67}Cu-F(ab′)$_2$ showed about half as much activity in the kidneys compared with ^{177}Lu-F(ab′)$_2$ (significance levels at 24 hours: P = 0.00049, 48 hours: P = 0.0153, and 72 hours: P = 0.0083). Tumor/kidney ratios at 24 hours were 0.76 ± 0.22 for ^{67}Cu-F(ab′)$_2$ and 0.38 ± 0.15 for the ^{177}Lu-F(ab′)$_2$ (significant

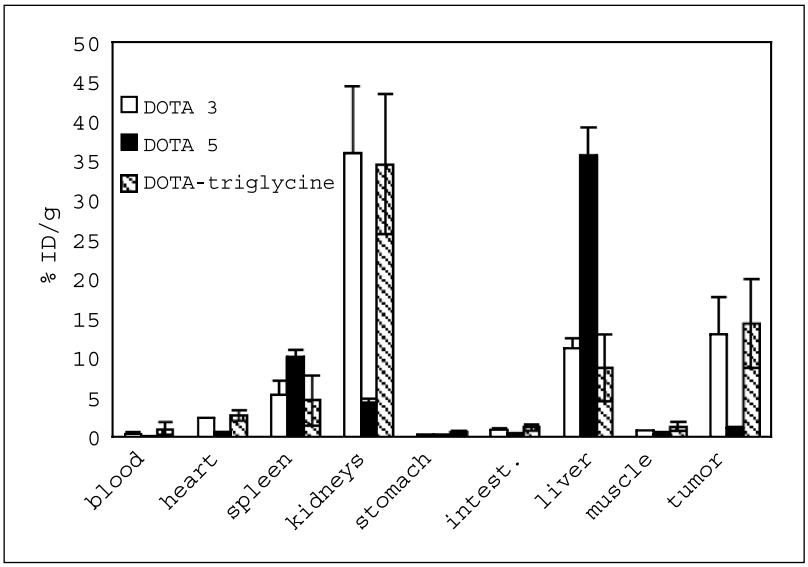

Fig. 2. Biodistributions 24 hours after injection of different ^{177}Lu-chCE7F(ab′)$_2$ conjugates (1.5-3.0 MBq, 13 μg) in tumor-bearing nude mice: effect of the number of chelators coupled to F(ab′)$_2$. White columns, ^{177}Lu-DOTA-chCE7F(ab′)$_2$ [five chelators/F(ab′)$_2$]; black columns, ^{177}Lu-DOTA-chCE7F(ab′)$_2$ [three chelators/F(ab′)$_2$]; striped columns, ^{177}Lu-DOTA-triglycine-chCE7F(ab′)$_2$ [two chelators/F(ab′)$_2$]. Data are %ID/g ± SD (n = 3) for the DOTA-conjugates (n = 8) for the DOTA-triglycine conjugate.

difference, P = 0.0005). Radioactivity in the liver was higher with the ^{67}Cu-F(ab′)$_2$ than with the ^{177}Lu-F(ab′)$_2$ at all of the time points. At 24 hours, differences were not significant (P = 0.243) but became significant at the 72-hour end point (P = 0.0311).

These results show that the biological behavior of the two conjugates, which were labeled with different metals via the same chelator, is different, especially regarding clearance of radioactivity from the kidneys.

Positron emission tomography imaging. PET imaging with intact ^{64}Cu-labeled chCE7 antibody fragments permitted excellent visualization of two different L1-CAM-expressing tumor models. Both s.c. SK-N-BE2c tumor xenografts and peritoneal metastases from human ovarian carcinoma SKOV3 cells were visualized with high resolution 21 hours after i.v. injection of 15 MBq ^{64}Cu-DOTA-triglycine-chCE7F(ab′)$_2$ (Fig. 4). Images showed low background, thus corresponding to the low blood activity levels and high tumor/blood ratios obtained in the biodistribution experiments (Table 4; Fig. 3). PET imaging with ^{64}Cu-DOTA-triglycine-chCE7F(ab′)$_2$ also served to investigate regional distribution of radioactivity in tumor and normal tissues with greater detail compared with classic biodistribution studies. In particular, previous PET imaging studies with the intact ^{64}Cu-chCE7 antibody revealed high accumulation of radioactivity in lymph nodes (33). In contrast, PET images of ^{64}Cu-labeled antibody fragments showed a lack of radioactivity uptake in lymph nodes. As expected from the biodistribution studies, high activity concentrations were found in the kidneys, the ultrahigh resolution of the Nano-PET camera showing inhomogeneous kidney uptake localized in the kidney cortex (Fig. 4B). Prominent uptake of radioactivity was also apparent in the liver. Regions of interest analysis of PET images resulted in tumor/kidney ratios of 1.2 and tumor/liver ratios of 0.9, being in line with the values determined in the biodistribution studies (Table 4). Furthermore, high-resolution PET imaging of the SK-N-BE2c tumor mass allowed the delineation of heterogeneous distribution of

Table 3. Biodistributions of ^{177}Lu-DOTA-triglycine-chCE7F(ab′)$_2$ in nude mice with human neuroblastoma (SK-N-BE2c) tumor xenografts

Tissue	2 h	4 h	8 h	24 h	48 h	72 h
Tumor	7.81 ± 1.86	9.54 ± 1.86	12.94 ± 3.67	14.43 ± 5.6	9.47 ± 1.70	7.56 ± 1.96
Blood	22.49 ± 1.10	10.89 ± 1.87	6.8 ± 0.96	1.00 ± 0.79	0.19 ± 0.06	0.28 ± 0.32
Heart	8.02 ± 1.88	4.57 ± 0.64	4.36 ± 0.9	2.71 ± 0.68	2.07 ± 0.64	1.57 ± 0.42
Spleen	6.79 ± 1.40	2.44 ± 0.52	4.91 ± 2.00	4.65 ± 3.15	5.20 ± 1.34	3.88 ± 2.02
Kidney	19.41 ± 1.75	15.05 ± 1.68	27.52 ± 5.95	34.48 ± 8.85	23.08 ± 8.04	17.22 ± 3.06
Stomach	1.02 ± 0.14	0.92 ± 0.43	1.16 ± 0.25	0.55 ± 0.25	0.47 ± 0.32	0.36 ± 0.11
Intestine	2.36 ± 0.24	1.78 ± 0.89	2.14 ± 0.32	1.24 ± 0.33	0.90 ± 0.22	0.73 ± 0.29
Liver	7.55 ± 0.60	5.89 ± 1.14	8.18 ± 2.15	8.70 ± 4.26	7.17 ± 1.47	5.44 ± 1.15
Muscle	1.64 ± 0.76	1.10 ± 0.37	1.75 ± 0.58	1.39 ± 0.56	2.12 ± 0.53	1.73 ± 0.81

NOTE: Groups of four mice were injected with 124 kBq (7.5 μg) ^{177}Lu-DOTA-triglycine-chCE7F(ab′)$_2$, and radioactivity in tumor and normal tissues was measured at the indicated time points. Data are presented as %ID/g ± SD (n = 4) and %ID/g ± SD (n = 8) for the 24-hour point.

Table 4. Biodistributions of ^{67}Cu-DOTA-triglycine-chCE7F(ab′)$_2$ in nude mice with human neuroblastoma (SK-N-BE2c) tumor xenografts

Tissue	2 h	4 h	8 h	24 h	48 h	72 h
Tumor	6.26 ± 0.87	6.43 ± 1.79	12.53 ± 2.39	11.92 ± 4.77	7.04 ± 2.02	5.31 ± 0.56
Blood	23.20 ± 2.48	12.86 ± 0.45	7.82 ± 0.89	2.30 ± 0.43	2.82 ± 0.18	1.93 ± 0.79
Heart	9.53 ± 0.56	7.42 ± 0.25	5.25 ± 0.65	2.92 ± 0.71	3.66 ± 0.39	4.09 ± 0.52
Spleen	5.07 ± 0.88	6.65 ± 0.61	6.26 ± 1.80	5.22 ± 1.73	4.21 ± 0.31	3.78 ± 0.84
Kidney	22.54 ± 2.73	28.10 ± 2.89	25.53 ± 5.51	16.00 ± 5.13	11.11 ± 2.27	8.75 ± 0.85
Stomach	1.11 ± 0.39	1.97 ± 0.39	2.18 ± 0.36	1.91 ± 1.17	1.57 ± 0.95	1.20 ± 0.04
Intestine	3.88 ± 0.18	5.14 ± 0.37	4.22 ± 0.62	3.56 ± 1.48	3.34 ± 0.47	5.8 ± 5.1
Liver	12.90 ± 4.96	16.79 ± 2.79	15.26 ± 5.56	11.12 ± 3.22	11.57 ± 1.87	9.90 ± 1.83
Muscle	1.62 ± 0.22	1.79 ±0.04	1.02 ± 0.32	0.91 ± 0.23	0.51 ±0.35	0.84 ± 0.07

NOTE: Groups of four mice were injected with 345 kBq (10 μg) ^{67}Cu-DOTA-triglycine-chCE7F(ab′)$_2$, and radioactivity in tumor and normal tissues was measured at the indicated time points. Data are presented as %ID/g ± SD (n = 4) and %ID/g ± SD (n = 9) for the 24-hour point.

radioactivity within the tumor. Figure 4C shows a series of coronal sections through the ovoid tumor, suggesting high vascularization and tracer perfusion even in the inner portions of the tumor. The images also suggest two areas within the tumor (arrows) with very low activity concentrations, probably representing necrotic tumor regions. Regions of interest analysis of these tumor subregions showed a 2.5-fold reduced tracer uptake in these putatively necrotic regions compared with average activity concentration in the residual tumor volume.

Dosimetry. ^{177}Lu-labeled chCE7F(ab′)$_2$ showed 2-fold higher radioactivity levels in the kidney and similar uptake of radioactivity in the liver compared with ^{67}Cu-chCE7F(ab′)$_2$ (Tables 3 and 4; Fig. 3). It was of interest to evaluate the effect of the different half-lives of the two nuclides on doses delivered to the kidneys and the liver. Dose calculations were done with pharmacokinetic data from Tables 3 and 4 using the OLINDA software (39). When taking the biological half-life of the conjugates into account, the calculated radiation burden of the (mouse) kidneys was 960 mGy/MBq for ^{67}Cu-F(ab)$_2$ and 2,000 mGy/MBq for ^{177}Lu-F(ab)$_2$. Doses for the liver were 850 and 690 mGy/MBq, respectively. The tumor was assumed to be a sphere of 0.5 g for which doses of 860 mGy/MBq ^{67}Cu and 1,050 mGy/MBq ^{177}Lu were obtained. If only the physical half-life of the radionuclides was considered for the time span 72 to 500 hours, a 20% higher dose was obtained for the ^{67}Cu conjugate, whereas for the corresponding ^{177}Lu compound the increase was 70%. The results show that due to the similar, rapid clearance of the ^{67}Cu and ^{177}Lu conjugates, the delivered dose is not significantly influenced by the longer physical half-life of ^{177}Lu.

Discussion

Clinical studies with the high-energy β^- particle–emitting nuclide ^{90}Y linked to anti-CD20 antibody ibritumomab showed that radioimmunotherapy with this radiopharmaceutical ("Zevalin") is a safe and effective treatment for patients with relapsed or refractory non-Hodgkin's lymphoma (40). For treatment of small metastases, medium-energy β^- particle emitters, such as ^{177}Lu or ^{67}Cu, may be more favorable due to their shorter effective path length and consequent sparing of normal tissues. Data from first patient studies with ^{177}Lu-labeled Rituximab (27) and preclinical studies with ^{177}Lu-labeled peptides (41) support this hypothesis. A further step toward optimizing the treatment of small metastases could be the introduction of antibody fragments labeled with ^{177}Lu or ^{67}Cu. To this purpose, we have engineered divalent fragments

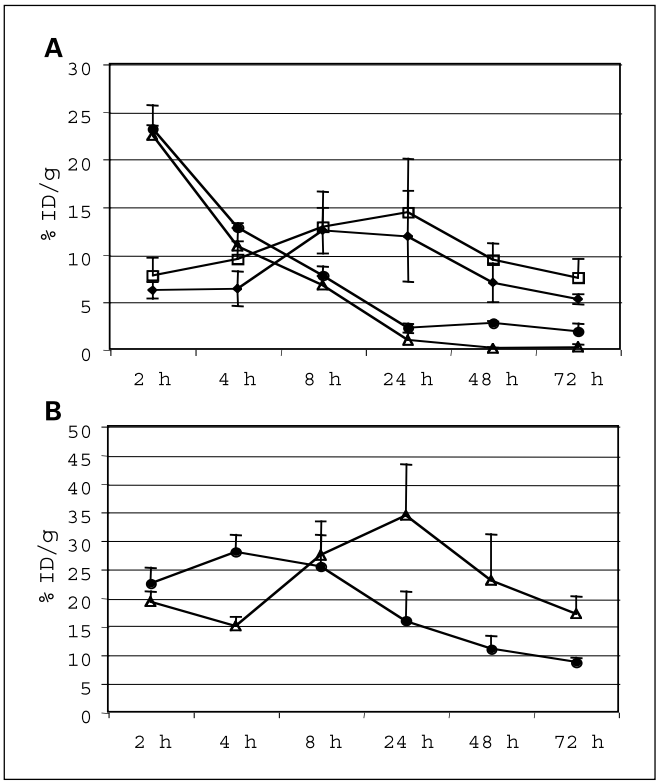

Fig. 3. Clearance of ^{177}Lu-DOTA-triglycine-F(ab′)$_2$ and ^{67}Cu-DOTA-triglycine-F(ab′)$_2$ from tumor, blood, and the kidneys. Corresponding numerical values are indicated in Tables 3 and 4. *A*, ●, ^{67}Cu-F(ab′)$_2$ blood; ◆, ^{67}Cu-F(ab′)$_2$ tumor; △, ^{177}Lu-F(ab′)$_2$ blood; □, ^{177}Lu-F(ab′)$_2$ tumor. *B*, ●, ^{67}Cu-F(ab′)$_2$ kidneys; △, ^{177}Lu-F(ab′)$_2$ kidneys.

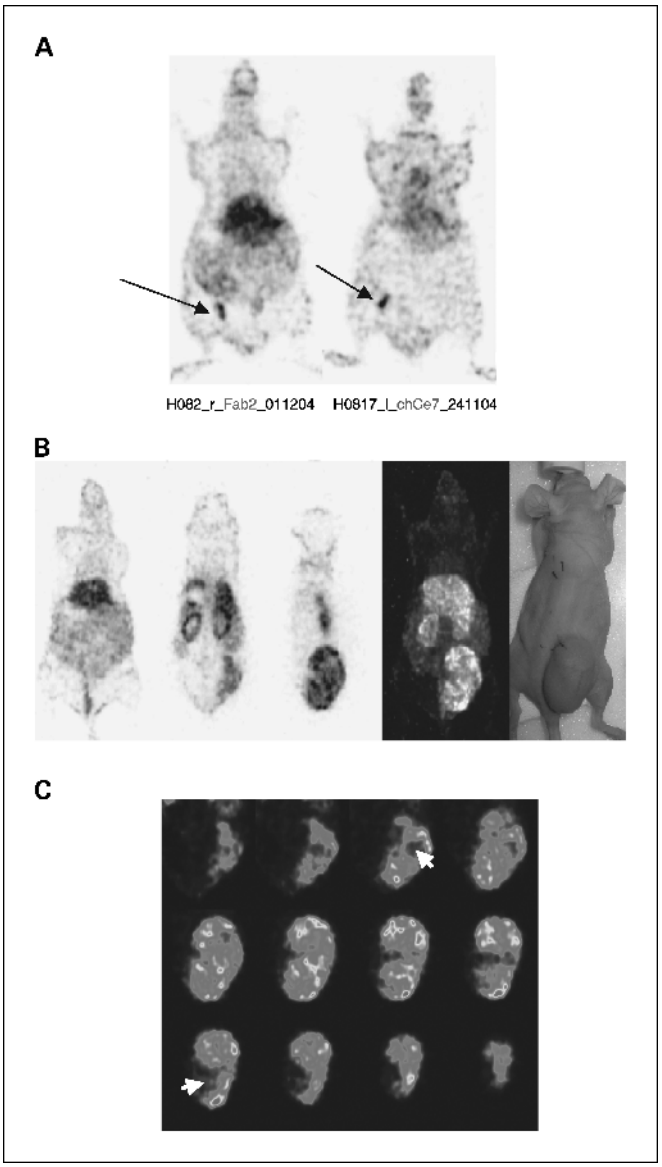

Fig. 4. PET imaging of tumor-bearing mice 21 hours after injection of ^{64}Cu-DOTA-triglycine-chCE7F(ab′)$_2$. *A*, comparative PET imaging of a mouse with a small peritoneal SKOV metastasis (*arrow*) injected with 20 MBq (100 μg) ^{64}Cu-chCE7 and 7 days later with 10 MBq (130 μg) ^{64}Cu-chCE7F(ab′)$_2$. Both whole body images show the same coronal plane through the tumor (slice thickness, 0.5 mm). *B*, PET imaging of a mouse with a SK-N-BE2c tumor (*right*) injected with 10 MBq (130 μg) ^{64}Cu-chCE7F(ab′)$_2$. The series of coronal whole body images show representative planes through the liver, kidneys, and tumor. The image to the right is the projection image. *C*, series of coronal slices with a more detailed view of tracer distribution within the tumor in *B* (*arrows* depicting putatively necrotic subregions).

of the internalizing anti-L1-CAM antibody chCE7 [F(ab′)$_2$ 110 kDa]. A comparison between ^{67}Cu- and ^{177}Lu-labeled fragments was done, because development of radiolabeled antibody fragments has to take into account availability of the chosen radionuclides in addition to good protein production yields and convenience of labeling protocols. Now, ^{177}Lu is more widely available than ^{67}Cu and has been successfully used for labeling of antibody fragments (9, 42) and peptides (29). In this study, almost identical procedures were used for radiolabeling with the two nuclides and fully immunoreactive fragments with similar specific activities were obtained. Maximal activity levels in tumors reached 12%ID/g to 14%ID/g at 24 hours for the ^{67}Cu- and ^{177}Lu-labeled antibody fragments. The kinetics of tumor uptake and clearance of radioactivity from the blood (Fig. 3) were slower than those observed for divalent diabodies (55 kDa). Pharmacokinetics were comparable with single-chain constructs engineered to dimerize via constant domain sequences, such as single-chain Fv-CH3 T84.66 (80 kDa; ref. 43) or single-chain Fv-CH4 L19 SIP (80 kDa; ref. 10) and also similar to CH2 domain–deleted antibodies CC49δCH2 (120 kDa; ref. 44). The tumor/blood ratios, which were reached at 24 hours, were 14.4 for the ^{177}Lu compound and 5.2 for the ^{67}Cu compound, which is lower than in the case of single-chain Fv–derived constructs labeled with radiometals.

Recombinant ^{67}Cu-F(ab′)$_2$ and ^{177}Lu-F(ab′)$_2$ conjugates were stable for at least 48 hours in human plasma, without evidence of degradation or aggregation (data not shown), indicating that the lower tumor/blood ratios are not due to circulating aggregates or metabolites. The clear PET images of both a large s.c. tumor and small-sized peritoneal metastases with ^{64}Cu-DOTA-triglycine-chCE7F(ab′)$_2$ (Fig. 4) indicate that tumor/blood ratios are sufficient for good imaging. Figure 4C shows heterogeneous uptake of radioactivity in the tumor xenograft and illustrates the value of PET imaging for exact dosimetry as opposed to measuring uptake values from overall tumor (or other organs, such as the kidney). The possibility to perform PET imaging may well represent an additional advantage of the radiocopper immunoconjugate as opposed to the lutetium conjugate.

Nontarget tissue uptake of radiometal-labeled immunoconjugates depends on the size of the constructs and the clearance properties of the labeled metabolites, which usually consist of the metal complexes linked to amino acid residues used for ligand coupling. It seems that single-chain constructs, such as diabodies, which are devoid of constant region sequences, show generally excessively high levels of radioactivity in the kidneys, similar to radiometal-labeled peptides. In contrast, some of the larger-sized immunoconjugates, which were tested in radiometal-labeled forms, showed better tumor/kidney ratios and sometimes considerable uptake of radioactivity in the liver and the spleen. In radiocopper-labeled F(ab′)$_2$ fragments, such as ^{64}Cu-CPTA-1A3F(ab′)$_2$ (31) and ^{67}Cu-CPTA-chCE7F(ab′)$_2$ (35), it was found that fragments labeled with positively charged copper complexes showed higher kidney uptake than fragments labeled with negatively charged copper complexes. A similar effect of charge on kidney uptake was observed in an octreotate conjugate labeled with ^{64}Cu using a cross-bridged macrocyclic chelator (45). For comparing ^{67}Cu and ^{177}Lu fragments, a DOTA-triglycine–linked chelator, which has been found previously to reduce kidney uptake of ^{67}Cu-F(ab′)$_2$ (32), was used and conjugation conditions were optimized. The main difference found between the conjugates consisted in 2-fold increased tumor/kidney ratios of the ^{67}Cu-DOTA-triglycine-F(ab′)$_2$. The negative charge of the Cu-DOTA complex may be responsible for reduced kidney uptake of the radiocopper-labeled conjugate as opposed to the neutral charge of the lutetium complex in the ^{177}Lu-labeled fragment. Apart from charge effects, our results show that biodistributions are

also strongly influenced by the number of ligands attached to antibody fragments as indicated by the data shown in Fig. 2, where protein substitution with increased molar excess of the DOTA ligand lead to ^{177}Lu immunoconjugates exhibiting loss of tumor uptake, a 7-fold reduction in kidney accumulation, and a 3.5-fold increase of liver uptake. Compared with an ^{111}In-DOTA-labeled T84.66 minibody with excellent tumor-targeting properties (43), liver uptake is lower with both ^{67}Cu- and ^{177}Lu-labeled chCE7F(ab′)$_2$. The strong uptake of radioactivity in lymph nodes we observed with ^{64}Cu-labeled chCE7 antibody (33) may be due to accumulation of radiolabeled metabolites in the reticuloendothelial system of the lymph nodes or to binding of the Fc region to activated lymphocytes and is not observed with ^{64}Cu-labeled chCE7 antibody fragments. We conclude that, with the exception of tumor/blood ratios, the tumor/tissue levels of the ^{67}Cu conjugate seem more favorable than those of the ^{177}Lu compound. Recently, we increased ^{67}Cu production to 15 GBq to provide therapeutic doses of ^{67}Cu-labeled intact antibodies. The results of this study suggest that the development of radiocopper-labeled antibody fragments is worthwhile both for PET imaging in ^{64}Cu-labeled form and for therapy in ^{67}Cu-labeled form.

Acknowledgments

We thank Susan Cohrs, Christine DePasquale, and Yvonne Eichholzer for excellent technical assistance.

References

1. Harris RJ, Shire SJ, Winter C. Commercial manufacturing scale formulation and analytical characterization of therapeutic recombinant antibodies. Drug Dev Res 2004;61:137–54.
2. Primiano T, Baig M, Maliyekkel A, et al. Identification of potential anticancer drug targets through the selection of growth-inhibitory genetic suppressor elements. Cancer Cell 2003;4:41–53.
3. Meli M, Carrel F, Waibel R, et al. Anti-neuroblastoma antibody chCE7 binds to an isoform of L1-CAM present in renal carcinoma cells. Int J Cancer 1999; 83:401–8.
4. Fogel M, Mechtersheimer S, Huszar M, et al. L1 adhesion molecule (CD171) in development and progression of human malignant melanoma. Cancer Lett 2003;189:237–47.
5. Fogel M, Huszar M, Altevogt P, et al. L1 (CD171) as a novel biomarker for ovarian and endometrial carcinomas. Expert Rev Mol Diagn 2004; 4:455–62.
6. Hoefnagel CA, Rutgers M, Buitenhuis CKM, et al. A comparison of targeting of neuroblastoma with mIBG and anti L1-CAM antibody mAb chCE7: therapeutic efficacy in a neuroblastoma xenograft model and imaging of neuroblastoma patients. Eur J Nucl Med 2001;28:359–67.
7. Wu AM, Yazaki PJ, Tsai S, et al. High-resolution micro-PET imaging of carcinoembryonic antigen-positive xenografts by using a copper-64-labeled engineered antibody fragment. Proc Natl Acad Sci U S A 2000; 2000:8495–500.
8. Wong YC, Chu DZ, Williams LE, et al. Pilot trial evaluating an ^{123}I-labeled 80-kilodalton engineered anticarcinoembryonic antigen antibody fragment (cT84.66 minibody) in patients with colorectal cancer. Clin Cancer Res 2004;10:5014–21.
9. Schott ME, Schlom J, Siler K, et al. Biodistribution and preclinical radioimmunotherapy studies using radiolanthanide-labeled immunoconjugates. Cancer 1994;73:993–8.
10. Borsi L, Balza E, Bestagno M, et al. Selective targeting of tumoral vasculature: comparison of different formats of an antibody (L19) to the ED-B domain of fibronectin. Int J Cancer 2002;102: 75–85.
11. Forero-Torres A, Khazaeli MB, Carpenter M, et al. Phase I trial of intravenous ^{131}I-HuCC49δCH2 in patients with metastatic colorectal carcinoma [abstract 730]. Proc Am Soc Clin Oncol 2003;22:82.
12. Juweid ME, Hajjar G, Swayne LC, et al. Phase I/II trial of ^{131}I-MN-14F(ab′)$_2$ anti-carcinoembryonic antigen monoclonal antibody in the treatment of patients with metastatic medullary thyroid carcinoma. Cancer 1999;85:1828–42.
13. Grünberg J, Knogler K, Waibel R, et al. High-yield production of recombinant antibody fragments in HEK-293 cells using sodium butyrate. Biotechniques 2003;34:968–72.
14. Novak-Hofer I, Amstutz HP, Maecke HR, et al. Cellular processing of copper-67-labeled monoclonal antibody chCE7 by human neuroblastoma cells. Cancer Res 1995;55:46–50.
15. Carrel F, Amstutz H, Novak-Hofer I, et al. Evaluation of radioiodinated and radiocopper labeled monovalent fragments of monoclonal antibody chCE7 for targeting of neuroblastoma. Nucl Med Biol 1997;24: 539–46.
16. Press OW, Shan D, Howell-Clark J, et al. Comparative metabolism and retention of iodine-125, yttrium-90, and indium-111 radioimmunoconjugates by cancer cells. Cancer Res 1996;56:2123–9.
17. Stein R, Chen S, Haim S, et al. Advantage of yttrium-90-labeled over iodine-131-labeled monoclonal antibodies in the treatment of a human lung carcinoma xenograft. Cancer Res 1997;80:2636–41.
18. Postema EJ, Frielink C, Oyen WJG, et al. Biodistribution of ^{131}I-, ^{186}Re-, ^{177}Lu-, and ^{88}Y-labeled hLL2 (Epratuzumab) in nude mice with CD22-positive lymphoma. Cancer Biother Radiopharm 2003;18: 525–33.
19. Deshpande SV, DeNardo SJ, Kukis D, et al. Copper-67 labeled monoclonal antibody Lym-1, a potential radiopharmaceutical for cancer therapy: labeling and biodistribution in RAJI-tumored mice. J Nucl Med 1988;29:217–25.
20. DeNardo GL, DeNardo SJ, Meares CF, et al. Pharmacokinetics of copper-67 conjugated Lym-1, a potential therapeutic radioimmunoconjugate, in mice and patients with lymphoma. Antibody Immunoconj Radiopharm 1991;4:777–85.
21. Connett JM, Anderson CJ, Baumann ML, et al. Cu-67 and Cu-64 labeled monoclonal antibody (mAb) as potential agents for radioimmunotherapy. J Nucl Med 1993;34:216P.
22. Smith A, Alberto R, Blaeuenstein P, et al. Preclinical evaluation of 67-Cu-labeled intact and fragmented anti-colon carcinoma monoclonal antibody mAb35. Cancer Res 1993;53:5727–33.
23. DeNardo SJ, DeNardo GL, Kukis DL, et al. 67-Cu-2IT-BAT-Lym-1 pharmacokinetics, radiation dosimetry, toxicity and tumor regression in patients with lymphoma. J Nucl Med 1999;40:302–10.
24. Bischof-Delaloye A, Delaloye B, Buchegger F, et al. Comparison of copper-67- and iodine-125-labeled anti-CEA monoclonal antibody biodistribution in patients with colorectal tumors. J Nucl Med 1997;38: 847–53.
25. DeNardo GL, DeNardo SJ, O'Donnell RT, et al. Are radiometal-labeled antibodies better than iodine-131-labeled antibodies: comparative pharmacokinetics and dosimetry of copper-67, iodine-131-, and yttrium-90-labeled Lym-1 antibody in patients with non-Hodgkin's lymphoma. Clin Lymphoma 2000;1:118–26.
26. Koppe MJ, Bleichrodt RP, Soede AC, et al. Biodistribution and therapeutic efficacy of $^{125/131}$I-, ^{186}Re-, $^{88/90}$Y-, or ^{177}Lu-labeled monoclonal antibody MN-14 to carcinoembryonic antigen in mice with small peritoneal metastases of colorectal origin. J Nucl Med 2004; 45:1224–32.
27. Forrer F, Lohri A, Uuijärvi H, et al. Radioimmunotherapy with lutetium-177-DOTA-Rituximab: a phase I/II-study in patients with follicular and mantle cell lymphoma. An interim analysis. Eur J Nucl Med Imaging 2003;30(Suppl2):76.
28. Bernhardt P, Ahlman H, Forsell-Aronson E. Model of metastatic growth valuable for radionuclide therapy. Med Phys 2003;30:3227–32.
29. Kwekkeboom DJ, Bakker WH, Kooij PP, et al. [^{177}Lu-DOTAOTyr3]octreotate: comparison with [^{111}In-DTPAo]octreotide in patients. Eur J Nucl Med 2001;28:1319–25.
30. Anderson CJ, Schwarz SW, Connett JM, et al. Preparation, biodistribution and dosimetry of copper-64-labeled anti-colorectal carcinoma monoclonal antibody fragments 1A3 F(ab′)$_2$. J Nucl Med 1995;36: 850–8.
31. Rogers BE, Anderson CJ, Connett JM, et al. Comparison of four bifunctional chelates for radiolabeling monoclonal antibodies with copper radioisotopes: biodistribution and metabolism. Bioconjug Chem 1996;7:511–22.
32. Zimmermann K, Gianollini S, Schubiger PA, et al. A triglycine linker improves tumor uptake and biodistributions of 67-Cu-labeled anti-neuroblastoma mAb chCE7 F(ab′)$_2$ fragments. Nucl Med Biol 1999;26: 943–50.
33. Zimmermann K, Gruenberg J, Honer M, et al. Targeting of renal carcinoma with 64/67-Cu-labeled anti L1-CAM antibody chCE7: PET imaging and selection of copper ligands. Nucl Med Biol 2003;30: 417–27.
34. Schwarzbach R, Zimmermann K, Blaeuenstein P, et al. Development of a simple and selective separation of ^{67}Cu from irradiated zinc for use in antibody labelling: a comparison of methods. Appl Radiat Isot 1995; 46:329–36.
35. Novak-Hofer I, Zimmermann K, Maecke HR, et al. Tumor uptake and metabolism of copper-67-labeled monoclonal antibody chCE7 in nude mice bearing neuroblastoma xenografts. J Nucl Med 1997;38: 536–44.
36. Lindmo T, Bunn PA Jr. Determination of the true immunoreactive fraction of monoclonal antibodies after radiolabeling. Methods Enzymol 1986;121: 678–91.
37. Rahmin A, Lenox M, Reader AJ, et al. Statistical list-mode image reconstruction for the high resolution

research tomograph. Phys Med Biol 2004;49: 4239–58.

38. Mikolajczyk K, Szabatin M, Rudnicki P, et al. A JAVA environment for medical image data analysis: initial application for brain PET quantitation. Med Inform (Lond) 1998;23:207–14.

39. Stabin MG, Siegel JA. Physical models and dose factors for use in internal dose assessment. Health Phys 2003;85:294.

40. Witzig TE, White CA, Gordon L, et al. Safety of Yttrium-90 ibritumomab tiuxetan radioimmunotherapy for relapsed low-grade, follicular, or transformed non-Hodgkin's lymphoma. J Clin Oncol 2003;21: 1263–70.

41. deJong M, Breeman WA, Valkema R, et al. Combination radionuclide therapy using ^{177}Lu- and ^{90}Y-labeled somatostatin analogs. J Nucl Med 2005;46: 13–7S.

42. Roberson PL, Yokoyama S, Rogers BE, et al. Three-dimensional dose model for the comparison of ^{177}Lu-HuCCdCH2 and ^{177}Lu-HuCC49 radioimmunotherapy in mice bearing intraperitoneal xenografts. Cancer Biother Radiopharm 2003;18:239–47.

43. Yazaki PJ, Wu AM, Tsai SW, et al. Tumour targeting of radiometal labelled anti-CEA recombinant T84.66 diabody and T84.66 minibody: comparison to radioiodinated fragments. Bioconjug Chem 2001; 12:220–8.

44. Slavin-Chiorini DC, Kashmiri SV, Schlom J, et al. Biological properties of chimeric domain-deleted anti-carcinoma immunoglobulins. Cancer Res 1995;55: 5957–67s.

45. Sprague JE, Peng Y, Sun X, et al. Preparation and biological evaluation of copper-64-labeled Tyr^3-octreotate using a cross-bridged macrocyclic chelator. Clin Cancer Res 2004;10:8674–82.

Clinical Cancer Research

In vivo Evaluation of ^{177}Lu- and $^{67/64}$Cu-Labeled Recombinant Fragments of Antibody chCE7 for Radioimmunotherapy and PET Imaging of L1-CAM-Positive Tumors

Jürgen Grünberg, Ilse Novak-Hofer, Michael Honer, et al.

Clin Cancer Res 2005;11:5112-5120.